Carbohydrate Polymers 121 (2015) 336–341

Contents lists available at ScienceDirect

Carbohydrate Polymers

journal homepage: www.elsevier.com/locate/carbpol

Prediction of mixed hardwood lignin and carbohydrate content using ATR-FTIR and FT-NIR

Chengfeng Zhou [a], Wei Jiang [b,*], Brian K. Via [a,c,*], Oladiran Fasina [c], Guangting Han [b]

[a] Forest Product Lab, School of Forestry and Wildlife Science, Auburn University, 520 Devall Dr., Auburn, AL 36849, USA
[b] Laboratory of New Fiber Materials and Modern Textile, The Growing Base for State Key Laboratory, Qingdao University, Qingdao 266071, PR China
[c] Department of Biosystems Engineering, Auburn University, Auburn, AL 36849, USA

ARTICLE INFO

Article history:
Received 17 April 2014
Received in revised form
18 November 2014
Accepted 26 November 2014
Available online 2 January 2015

Keywords:
Chemical composition
Fast prediction
ATR-FTIR
FT-NIR
Hardwood

ABSTRACT

This study used Attenuated total reflectance Fourier transform infrared (ATR-FTIR) spectroscopy and Fourier transform near-infrared (FT-NIR) spectroscopy with principal component regression (PCR) and partial least squares regression (PLS) to build hardwood prediction models. Wet chemistry analysis coupled with high performance liquid chromatography (HPLC) was employed to obtain the chemical composition of these samples. Spectra loadings were studied to identify key wavenumber in the prediction of chemical composition. NIR–PLS and FTIR–PLS performed the best for extractives, lignin and xylose, whose residual predictive deviation (RPD) values were all over 3 and indicates the potential for either instrument to provide superior prediction models with NIR performing slightly better. During testing, it was found that more accurate determination of holocellulose content was possible when HPLC was used. Independent chemometric models, for FT-NIR and ATR-FTIR, identified similar functional groups responsible for the prediction of chemical composition and suggested that coupling the two techniques could strengthen interpretation and prediction.

1. Introduction

As the most abundant fibrous material, wood is utilized in numerous areas including textiles (Mak, Yuen, Ku, & Kan, 2006), paper making (Weinstock et al., 1997), building construction (Ellingwood, Rosowsky, Li, & Kim, 2004), composites (Ruffing, Shi, Brown, & Smith, 2011) and bioenergy (Celikbag, Via, Adhikari, & Wu, 2014). The key bio-based polymers for wood are cellulose, hemicellulose and lignin. The chemical composition of wood plays an important role when one evaluates the utility of a feedstock for various product streams. Rapid assessment of biomass would allow for better categorization of raw materials for end use, allow for better process control, and assist in genetic selection of superior trees. Wet chemistry methods are currently still preferred to yield accurate and precise results. But wet methods are complex and consume many chemicals over long periods of time. Moreover, chemical modification of the fiber can destroy the wood matrix which is unacceptable for some studies. The slower time to testing also limits the sample size that one can measure in a short period of time (Ferraz, Baeza, & Durán, 1991; Jiang, Han, Zhang, & Wang, 2010; Kaar & Brink, 1991).

Fourier transform near-infrared (FT-NIR) spectroscopy possesses unique advantages, such as being fast, nondestructive, simple and low in cost (Roggo et al., 2007; Tsuchikawa, 2007). More recently, FT-NIR models were found to be suitable for the analysis of the chemical composition of wood (Chen et al., 2010; Raymond & Schimleck, 2002; Via, Shupe, Groom, Stine, & So, 2003), corn stover (Philip Ye et al., 2008), rice straw (Jin & Chen, 2007) and tobacco (Zhang, Cong, Xie, & Zhao, 2008). These studies utilized both principal component regression (PCR) and partial least squares regression (PLS) to calibrate to the NIR spectra. It was found that PLS performed better than PCR when dealing with low detection-limit samples (Lipp, 1996), while PCR could yield simple and better models for cases where interpretation of the model was important (Jouan-Rimbaud, Walczak, Massart, Last, & Prebble, 1995; Via, Zhou, Acquah, Jiang, & Eckhardt, 2014).

Like FT-NIR, FTIR has the potential to predict with high accuracy and precision but often comparisons are limited (Chen et al., 2010; Schultz & Burns, 1990). For pharmaceutical applications, FTIR

* Corresponding authors at: Forest product lab, School of Forestry and Wildlife Science, Auburn University, 520 Devall Dr., Auburn, AL 36849, USA and Laboratory of New Fiber Materials and Modern Textile, The Growing Base for State Key Laboratory, Qingdao University, Qingdao 266071, PR China.
Tel.: +86 532 83780377/+1 334 844 1088; fax: +86 532 83780377/+1 334 844 1084..
E-mail addresses: chengfengzhou828@gmail.com (C. Zhou), weijiangqd@gmail.com (W. Jiang), BKV0003@auburn.edu (B.K. Via), fasinoo@auburn.edu (O. Fasina), Kychgt@qdu.edu.cn (G. Han).

http://dx.doi.org/10.1016/j.carbpol.2014.11.062
0144-8617/

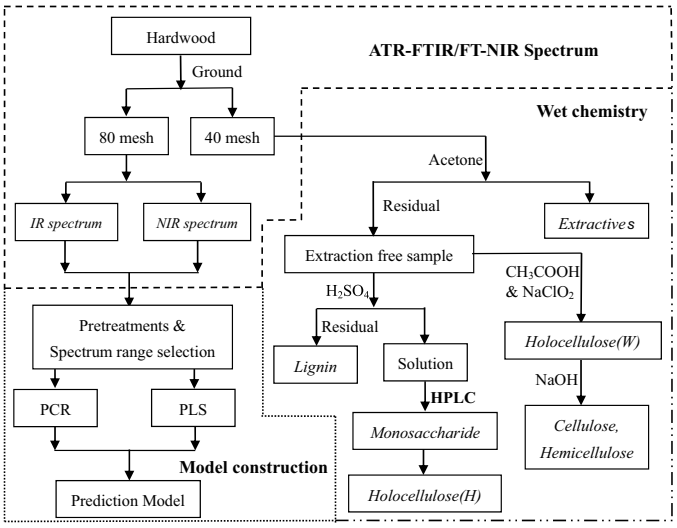

Fig. 1. Schematic diagram for wet chemistry and ATR-FTIR/FT-NIR model construction.

was found to perform better than FT-NIR for the classification of five different cellulosic materials (Langkilde & Svantesson, 1995). It was also demonstrated that FT-IR performed better for the determination of soil properties (Rossel, Walvoort, McBratney, Janik, & Skjemstad, 2006). To date, the comparison of techniques for wood based materials is limited to studies that utilize less robust multivariate techniques (Schultz & Burns, 1990).

This research aimed to evaluate the ability to build calibration equations for ATR-FTIR and FT-NIR using different regression techniques for the hardwood chemistry of several commercially important genus/species. Interpretation of PLS and PCR loadings was also performed to assess model quality.

2. Experimental

2.1. Sample preparation

All samples were collected from newly harvested hardwood trees. There were 4 different genus/species to generate 37 samples in which 4 Eucalyptus, 9 cotton wood, 12 aspen and 12 poplar were used for testing. First, the solid wood samples were planed down to 3 mm thick wood chips (about 100 g), and then placed in ambient conditions (23–26 °C and less than 50% humidity) for 2 weeks to evaporate free water within the cell lumen. Then 50 g of the air dried samples were ground to 40 mesh using a Willey mill and then 20 g of 40 mesh samples were further ground to 80 mesh. The 40 mesh samples were used for wet chemistry analysis and 80 mesh samples were used for ATR-FTIR and FT-NIR spectra collection. Grinding these samples to a fine mesh was considered important since the porosity of solid materials can influence the reflectance of light (Dutta, Raghavan, & Ngadi, 2012) resulting in higher errors during prediction (Jiang et al., 2014a; Jiang, Via, Han, Wang, & Liu, 2014b).

2.2. Wet chemistry analysis

The extractives, lignin, and monosaccharide content of 37 samples were measured on the basis of standard procedures developed by the National Renewable Energy Laboratory (NREL) (Sluiter et al., 2008). The cellulose, hemicellulose, and holocellulose contents were also measured by traditional wet chemistry analysis. As shown in Fig. 1, 150 mL acetone was used to extract 5 g of sample for 6 h to get acetone extractives. After extractive removal, the extractive free sample was separated into 2 batches.

Batch 1: A 72% (w/w) sulfuric acid treatment at 30 °C for 2 h was used to prehydrolyze the extractive free sample. The solution was then diluted to 4% sulfuric acid with distilled water, sealed in a bottle, and placed in an autoclave for 1 h at 121 °C, and then the residual from the bottle was filtered and oven dried to measure the lignin content. The extractives and lignin contents were measured by gravimetric analysis. To determine the monosaccharide composition (glucose, xylose, etc.), an HPLC (Shimadzu LC-20A), equipped with an Aminex 87 P column and differential refractive index detector, was employed to analyze the sugar solution. Holocellulose content (Holo-HPLC) was calculated as the sum of all the monosaccharides contents.

Batch 2: Delignification treatments were conducted to determine the holocellulose content. The delignification procedure was as follows. First, 2 g was weighed separately and placed into conical flasks (500 mL) with 320 mL distilled water in each flask. Second, the sample was placed in flasks and the flasks were then placed into a water bath (75 °C), and then 1 mL of acetic acid (ACS grade, 100%) and 20 mL 15% (w/w) sodium chlorite were added into each flask every 1 h. After 4 h water bath exposure, the residues were filtered with filter paper and then oven dried for 3 h to test the holocellulose content. After the holocellulose content was determined, 1.5 g of oven dried holocellulose was placed into a 250 mL conical flask. One-hundred milliliter of 17.5% sodium hydroxide was then added and the air in the flask was replaced with nitrogen and the flask was sealed with aluminum foil. Following the flask was placed in a water bath at 20 °C and stirred occasionally until the reaction was complete. Then the solution was filtered through a pre-weighed filter paper and washed with distilled water (at least 500 mL). The sample was then oven dried at 105 °C overnight and weighed. The residue was determined as cellulose and the hemicellulose content was considered to be the difference in holocellulose and cellulose.

When conducting wet chemistry, all samples were air dried and tested for moisture content to calculate the dry weight of the original samples. All experiments were performed in duplicate. All chemicals were purchased from the VWR Company and they were all analytically pure or even chromatographically pure.

2.3. ATR-FTIR and FT-NIR acquisition

Spectra from both instruments were acquired from 80 mesh wood samples and all samples were oven dried overnight prior to analysis. For each sample, the wood powder was placed on the diamond (ATR-FTIR) or light path (FT-NIR) and the reflectance spectra were collected. The PerkinElmer spectrum 400 FT-IR/FT-NIR spectrometer was utilized to collect the mid and near infrared spectra. For FT-NIR, the spectrum covered a range of 10,000–4000 cm^{-1} with a spectral resolution of 4 cm^{-1}. Each spectrum was collected from an average of 32 scans. For the ATR-FTIR, the spectrum covered a range of 4000–650 cm^{-1} with a spectral resolution of 4 cm^{-1}. The pressure of the ATR-FTIR acquisition was 70 ± 2 psi. Each spectrum was collected from an average of 4 scans.

2.4. Chemometric analysis

Spectrum Quant + software was used for model construction. PCR and PLS were the two statistical methods used to build ATR-FTIR and FT-NIR models. These methods allowed for the optimal estimation of the y value from the spectral data matrix. These two modeling methods were further combined with different pretreatments such as first derivative (FD), offset, flat, multiplication scattering correction (MSC) and standard normal variate (SNV). Thirty-two samples were used to construct models and 5 samples were used for validation. Leave one out cross validation was also ran to ensure similar results to the validation data set. The predictive performance of the models in this paper was evaluated by several

Table 1
Statistical summary of components in wood analyzed with wet chemistry and HPLC methods.

Chemical composition	Mean value of content (%)	Range of content (%)	SD value
Extractives	2.11	0.66–5.93	1.42
Lignin	26.24	20.85–31.63	2.41
Cellulose	43.71	39.84–49.05	2.10
Hemicellulose	35.97	28.35–43.12	3.88
Holocellulose	79.68	71.52–84.66	3.49
Holo-HPLC[a]	64.52	57.85–68.64	2.37
Glucose	44.34	40.90–47.06	1.31
Xylose	16.69	13.76–20.31	1.56
Total (*W*)[b]	108.03	101.49–113.07	N/A
Total (*H*)[c]	92.88	87.36–98.38	N/A

[a] Holo-HPLC represents the holocellulose content calculated from HPLC results.
[b] Total (*W*) represents the total content that was calculated from wet chemistry. Total (*W*) = extractives + lignin + holocellulose.
[c] Total (*H*) represents the total content that was calculated from HPLC. Total (*H*) = extractives + lignin + holo-HPLC.

Table 2
RMSEP value of components in wood analyzed with different methods.

Chemical composition	FT-NIR		ATR-FTIR	
	PCR	PLS	PCR	PLS
Extractives	0.80	0.37	0.69	0.49
Lignin	0.87	0.46	0.83	0.84
Cellulose	2.00	1.79	4.03	3.20
Hemicellulose	1.53	0.97	1.61	2.00
Holocellulose	1.94	1.69	2.43	2.60
Holo-HPLC	1.59	1.29	1.76	1.61
Glucose	0.85	0.63	0.69	0.90
Xylose	0.72	0.46	0.68	0.62

standards, including correlation coefficient (*r*), root mean square error of calibration (RMSEC), root mean square error of prediction (RMSEP) and residual predictive deviation (RPD).

$$\mathrm{RPD} = \sqrt{\frac{\sum_{i=1}^{n}\left(C_i - \bar{C}_i\right)^2}{n-1}}/\mathrm{RMSEP}. \quad (1)$$

where C_i is the wet chemistry value in the validation; $\bar{C}_i$ is the mean of the wet chemistry value in the validation; n is the number of samples in the validation. In this research, the RPD value was calculated from Tables 1 and 2. A good model should have a high *r*, a high RPD, and a low RMSEC, RMSEP.

3. Results and discussion

3.1. Wet chemistry and HPLC analysis results

Two methods (Batch 1: HPLC and Batch 2: wet chemistry) were used to determine the carbohydrates content. The results for both methods were found to be systematically different during the measurement of holocellulose. As shown in Table 1, after using wet chemistry analysis, the range in lignin content was 20.85–31.63%, cellulose content (39.84–49.05%), hemicellulose content (28.35–43.12%) and holocellulose content (71.52–84.66%). These findings were statistically similar to other studies demonstrating a representative sample (Pettersen, 1984). However, the range of the total (*W*) content (101.49–113.07%) was higher than 100%, which implied that some experimental error existed. The error was considered to be some portion of lignin which was not completely removed in the delignification treatment (Kačík, Ďurkovič, & Kačíková, 2012). The lignin was counted as holocellulose, which resulted in the inaccuracy of holocellulose content. More recently, HPLC was widely used to analyze carbohydrates,

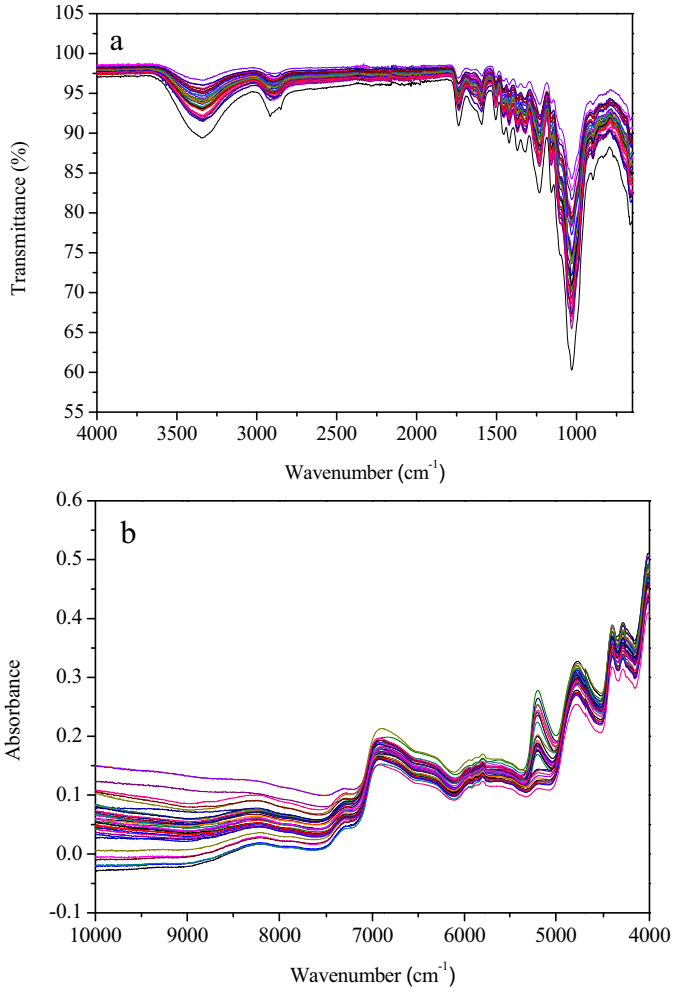

Fig. 2. ATR-FTIR (a) and FT-NIR (b) spectra used for the predictions.

but minute degradation of some monosaccharides during HPLC processing can occur resulting in a mass balance below 100% ((Li & Xu, 2013; Oliver, Gaborieau, Hilder, & Castignolles, 2013). Moreover, there are a few proteins and uronic acids that commonly exist (Sluiter et al., 2008), which were unidentifiable with our HPLC equipment and resulted in Total (*H*) (87.36–98.38%) values less than 100% (Table 1). Nevertheless, the holocellulose that was determined from HPLC was hypothesized to be closer to the real value than that from wet chemistry. In this research, both holocellulose content (holocellulose/Holo-HPLC) and other carbohydrate contents (hemicellulose, cellulose, glucose and xylose) were used for NIR model training.

3.2. ATR-FTIR and FT-NIR multivariate models

As described above, multivariate models for wood chemical composition were established from ATR-FTIR and FT-NIR spectra (Fig. 2a and b) coupled with PLS and PCR algorithms. This resulted in 4 different prediction models for each chemical component (Figs. 3 and 4). As shown in Figs. 3 and 4, the PLS model coupled with FT-NIR spectroscopy almost always showed the best prediction accuracy, except for xylose in which ATR-FTIR–PLS was statistically similar in *r* value. Schultz and Burns (1990) also found NIR based models to provide better prediction errors than FTIR when KBr pellets were used. Similar results were also found when predicting feedstock strand density in which FT-NIR performed better than ATR-FTIR (Via, 2010). The *r* values for all components of the

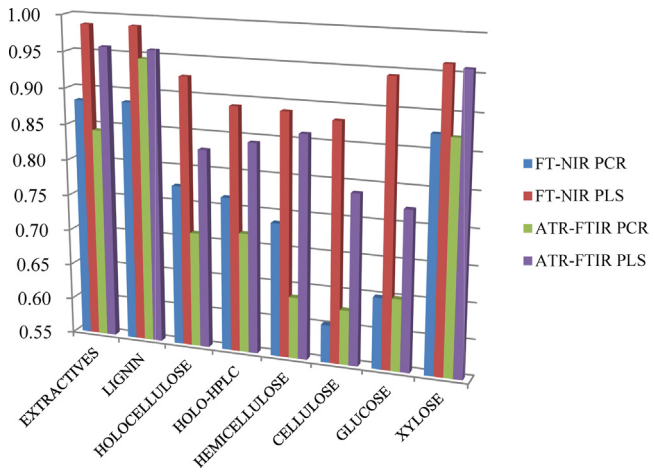

Fig. 3. *r* Values for each chemistry component in wood that was analyzed using FT-NIR and ATR-FTIR and different modeling methods.

FT-NIR–PLS model were over 0.85; and the RPD values were all greater than 1.5. RPD values in this range suggest that FT-NIR–PLS can be used for screening purposes during quality control of individual samples (Yeh et al., 2005). However, individual samples are generally not the primary metric of interest during production, but instead population parameters such as production mean and variance are more important indicators of process capability (Via, Adhikari, & Taylor, 2013). These parameters can be estimated with accuracy despite only modest RPD values (Sjoblom, Johnsson, & Sundstrom, 2004).

The best predictive results for the FT-NIR–PLS model occurred for extractives, lignin and xylose in which the *r* values for these three models were greater than 0.95, and the RPD values were higher than 3. The greater RPD values for these prediction models suggest that FT-NIR may be more useful than just screening. Other researchers support that models were considered good enough to monitor the quality of individual samples when the *r* was >0.90 and the RPD was >3 (Fagan, Everard, & McDonnell, 2011; Williams & Sobering, 1993). Of these two, lignin based models exhibited the best performance in which 96% of the overall variation was accounted for during calibration and this predictive capacity held up during validation with minimum degradation in RMSEP.

The higher RPD values suggest that FT-NIR–PLS prediction models for extractives, lignin and xylose can be used for quantitative analysis of specific samples in a laboratory or manufacturing

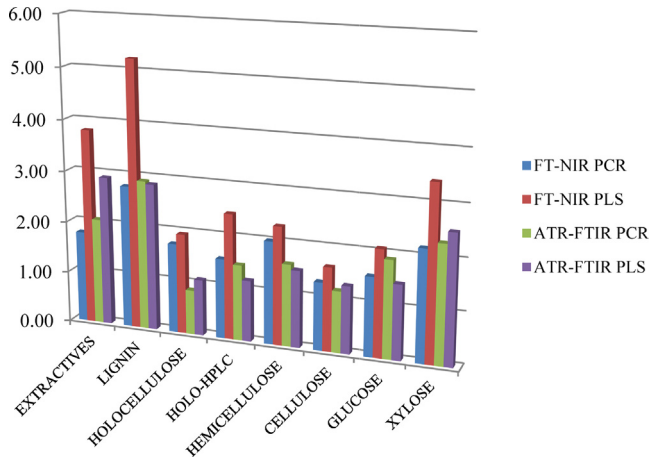

Fig. 4. RPD values for each chemical component in wood that was analyzed using FT-NIR and ATR-FTIR and different modeling methods.

setting. The good prediction diagnostics for extractives and lignin content could be partially explained by their considerable difference from carbohydrates. Carbohydrates, including cellulose, hemicellulose and holocellulose form polysaccharides which contain monosaccharides such as glucose, xylose, and other sugars. These sugars are more similar than they are different with only slight variations in the location of H and OH groups with respect to the cyclical 6 carbon hexagonal monomer structure. And this may result in error when trying to differentiate between different sugar types using chemometric models on ATR-FTIR or FT-NIR spectra.

This study found that PCR performed similarly to their study in which they used MLR models to account for 73% of the variation in hemicellulose concentration. But when PLS was used in this study, the models accounted for 88% of the variation during calibration. Likewise, when the remaining models were evaluated, PLS consistently accounted for more variation in wood chemistry than in PCR. The RPD values were also consistently the highest for PLS for both ATR-FTIR and FT-NIR systems (Fig. 3). However, only the FT-NIR models coupled with PLS achieved RPD values greater than 3, while the remaining models and respective chemical constituents were below 3 and could thus only be useful for screening.

Most models built for ATR-FTIR were below 2 and some even less than 1.5. These findings support that ATR-FTIR based models generally fall within the screening capacity for most wood chemistry or monomer based sugars. With some exception, ATR-FTIR models did perform reasonably strong for lignin, extractives, and xylose (Figs. 3 and 4). This was compatible to FT-NIR which also showed the highest predictive capacity for these three dependent variables.

In this research, ATR-FTIR and FT-NIR models were calibrated on measurements made from wet chemistry and HPLC. The RPD values of Holo-HPLC based models performed better than when the data was obtained from wet chemistry. This suggests that HPLC provides better accuracy and precision than wet chemistry based methods for sugar and hemicellulose estimation.

3.2.1. *Interpretation of FT-NIR and ATR-FTIR models*

Combining multivariate modeling with two instruments can provide additional insight in that similar band assignments for both ATR-FTIR and FT-NIR may be found for a given perturbation. Such agreement between models and instruments provides additional confidence that the right independent parameters were chosen for the model. Multiple instruments can further aid in the interpretation of key mechanisms that contribute to the prediction of a chemical constituent. Table 3 provides a summary of key band locations in both the near and mid infrared region in the prediction of wood chemistry. For most models, there was no clear trend as to which modeling technique worked better for interpretation. PCR appeared to work as well as PLS when assigning bands and making interpretations. This suggests that PCR is more comparable to PLS if the goal is to interpret the effect of underlying mechanisms on the *y* variable of interest. However, if ranking of statistical variables through statistical hypothesis testing is important, PCR may be preferred over PLS (Via, 2010; Via et al., 2013). During the prediction of density with ATR-FTIR, it was found that PCR worked better than multiple linear regression (Via, Fasina, & Pan, 2011). The current study suggests that PLS could be used as a substitute for PCR when interpreting models. But care should be taken since the loading bands can differ due to error during estimation (Via et al., 2014). This may be useful since many studies prefer PLS modeling due to better prediction diagnostics as witnessed in this study. In summary, it has been shown that when many studies in other scientific fields were observed, PCR generally outperformed PLS for interpretation while PLS was better for prediction of the *y* variable (Senter, 2008; Via et al., 2014).

Table 3
Significant wavenumber extracted from PLS and PCR modeling for the prediction of wood chemistry and monosaccharides for FT-NIR and ATR-FTIR.

Chemical constituent	FT-NIR		FT-NIR band location	Band assignment	ATR-FTIR		ATR-FTIR band location	Band assignment
	PCR	PLS			PCR	PLS		
Extractives	5205	5197	5220-5150	O—H asym. str. + O—H def. of H_2O	1269	1269	1271	C—O
	5994	5961	5995	C-H str.	1506	1508	1510	C—C or C=C
					1636	1640	1633	
	–	–	–	–	1733	1732	1730	C=O str
Lignin	4412	4417	4411	O—H str. + C—O str.	833	833	835	O—H or C—H def.
					1374	1375	1375	
	5986	5981	5980	C—H str.				
	–	–	–	–	1023	1011	1033	Aromatic C—H def. + C—O def. + C=O str.
					1124	1126	1116	
	–	–	–	–	1214	1211	1220	C—C + C—O + C=O str.
	–	–	–	–	1326	1323	1328	C=O str.
					1734	1731	1735	
	–	–	–	–	1505	1503	1510	C—C + C=C
Cellulose	4412	4412	4405	O—H str. + C—O str.	1234	1187	1235–1225	O—H def.
Hemicellulose	–	–	–	–	1019	1029	1120–1000	Carb.
	–	–	–	–	1059	1072	1051	C—O—C str.
	–	–	–	–	1263	1260	1267	C—H_2
	–	–	–	–	1419	1423	1426	C—H + O—H bend.
	–	–	–	–	1507	1509	1509	C—C + C=C
	–	–	–	–	1633	1604	1639	Water
Glucose	–	–	–	–	1026	1044	1025	C—O or C—C vibration
					1137	1137	1149	
	–	–	–	–	1221	1188	1203	C—H or O—H
					2922	2922	2913	
	–	–	–	–	1462	1456	1460	C—H_2 + O—C—H + C—C—H

sym.: symmetric, asym.: antisymmetric, str.: stretching vibration, bend.: bending vibration, def.: deformation vibration, carb.: carbohydrates.

In this study, for the prediction of extractives content, the C—H, C—C and C=C stretch were important loadings (Table 3). For lignin, the O—H and C—H bond were common to both instruments, while C=O was important for ATR-FTIR. For cellulose prediction, the O—H deformation was key functional groups identified by both techniques, but C—O was vital to FT-NIR. Hemicellulose quantification was perhaps the most different with the band assignment. The difference in models in the prediction of hemicellulose may be beneficial and suggests that both instruments might be combined to yield better predictive capacity. This may be important since, in this study, the prediction of hemicellulose was more difficult than other wood polymers with lower predictive capability. It is thus no surprise that these same differences between instruments were also observed during the modeling of glucose (Table 3).

It should finally be noted that the FT-NIR and ATR-FTIR bands listed in Table 3 were obtained through PCR and PLS modeling and may differ from some assignments found in the literature through similar or other methods. Fig. 5 shows an example a loading plot for PCR and PLS models for lignin content. Two bands were assigned to lignin from the literature (4411 and 5980 cm^{-1}) (Schwanninger, Rodrigues, & Fackler, 2011). When the PCR and PLS models were built and loadings compared, for lignin, the models overestimated the wavenumber by as much as 6 cm^{-1} (Fig. 5). When the loadings for all chemistry models were compared for FT-NIR, most values fell within ±5 from common literature based assignments, but in several cases was as high as ±10 (Table 3) and in a few cases as high as ±20. Similar errors for ATR-FTIR chemometric models were also present for the biopolymers explored in this study. This new finding suggests that consideration for model errors in loading estimates is important when assigning wavelengths to biopolymer concentration if one is to avoid misleading conclusions during band assignment or interpretation.

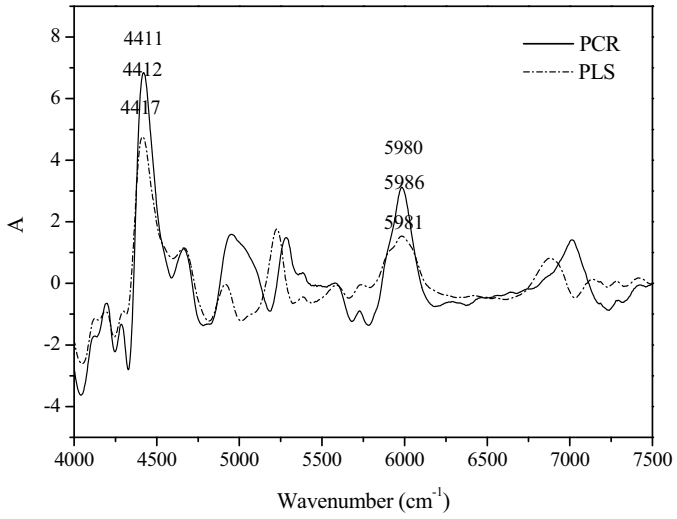

Fig. 5. A comparison of PCR and PLS loadings (raw spectra) for the prediction of lignin with FT-NIR spectroscopy. The wavenumber of two important bands were placed within the graph in which the top number represents values extracted from the literature, the middle number represents the loading value obtained through PCR and the bottom number represents that obtained through PLS.

4. Conclusions

The chemical composition of extractive, lignin, cellulose, hemicellulose, holocellulose, glucose and xylose in hardwood were determined using wet chemistry and HPLC. Prediction models were built for these chemical compositional components using PLS and PCR with ATR-FTIR and FT-NIR spectra. It was found that using HPLC can get the more accurate holocellulose content measurements

than when using the wet chemistry methods. ATR-FTIR spectra can be used for screening purposes while FT-NIR often could be used for monitoring the quality of specific samples. PLS performed best during the prediction chemical composition with the best prediction models being extractive, lignin and xylose. PCR worked as good as PLS if interpretation of the model was important. It was also found that FT-NIR and ATR-FTIR models could be compared to gain additional insight into the effect of functional groups on chemical composition prediction.

Acknowledgments

This work was most supported by the Agriculture and Food Research Initiative (AFRI) CAP—"Southeast Partnership for Integrated Biomass Supply Systems"; the Department of Energy grant titled, "High Tonnage Forest Biomass Production Systems from Southern Pine Energy Plantations". Other smaller contributions included the Hatch in which these calibration equations will be utilized to partition out feedstocks of high lignin for adhesive production, Regions Bank; the National Natural Science Foundation of China (50973048); National Natural Science Foundation of Shandong Province (ZR2012EM002); Special Foundation of "Taishan Scholar" Construction and National Science & Technology Pillar Program (2012BAD32B06).

Appendix A. Supplementary data

Supplementary data associated with this article can be found, in the online version, at http://dx.doi.org/10.1016/j.carbpol.2014.11.062.

References

Celikbag, Y., Via, B. K., Adhikari, S., & Wu, Y. (2014). Effect of liquefaction temperature on hydroxyl groups of bio-oil from loblolly pine (*Pinus taeda*). *Bioresource Technology*, *169*, 808–811.

Chen, H., Ferrari, C., Angiuli, M., Yao, J., Raspi, C., & Bramanti, E. (2010). Qualitative and quantitative analysis of wood samples by Fourier transform infrared spectroscopy and multivariate analysis. *Carbohydrate Polymers*, *82*(3), 772–778.

Dutta, B., Raghavan, G., & Ngadi, M. (2012). Surface characterization and classification of slow and fast pyrolyzed biochar using novel methods of pycnometry and hyperspectral imaging. *Journal of Wood Chemistry and Technology*, *32*(2), 105–120.

Ellingwood, B. R., Rosowsky, D. V., Li, Y., & Kim, J. H. (2004). Fragility assessment of light-frame wood construction subjected to wind and earthquake hazards. *Journal of Structural Engineering*, *130*(12), 1921–1930.

Fagan, C. C., Everard, C. D., & McDonnell, K. (2011). Prediction of moisture, calorific value, ash and carbon content of two dedicated bioenergy crops using near-infrared spectroscopy. *Bioresource Technology*, *102*(8), 5200–5206.

Ferraz, A., Baeza, J., & Duránt, N. (1991). Softwood biodegradation by an ascomycete *Chrysonilia sitophila* (TFB 27441 strain). *Letters in Applied Microbiology*, *13*(2), 82–86.

Jiang, W., Han, G., Via, B., Tu, M., Liu, W., & Fasina, O. (2014). Rapid assessment of coniferous biomass lignin–carbohydrates with near-infrared spectroscopy. *Wood Science and Technology*, *48*(1), 109–122.

Jiang, W., Han, G., Zhang, Y., & Wang, M. (2010). Fast compositional analysis of ramie using near-infrared spectroscopy. *Carbohydrate Polymers*, *81*(4), 937–941.

Jiang, W., Via, B. K., Han, G., Wang, Q., & Liu, S. (2014). Near infrared monitoring of untreated and chemically delignified wood. *Journal of Near Infrared Spectroscopy*, *21*(6), 485–493.

Jin, S., & Chen, H. (2007). Near-infrared analysis of the chemical composition of rice straw. *Industrial Crops and Products*, *26*(2), 207–211.

Jouan-Rimbaud, D., Walczak, B., Massart, D., Last, I., & Prebble, K. (1995). Comparison of multivariate methods based on latent vectors and methods based on wavelength selection for the analysis of near-infrared spectroscopic data. *Analytica Chimica Acta*, *304*(3), 285–295.

Kaar, W. E., & Brink, D. L. (1991). Summative analysis of nine common North American woods. *Journal of Wood Chemistry and Technology*, *11*(4), 479–494.

Kačík, F., Ďurkovič, J., & Kačíková, D. (2012). Chemical profiles of wood components of poplar clones for their energy utilization. *Energies*, *5*(12), 5243–5256.

Langkilde, F., & Svantesson, A. (1995). Identification of celluloses with Fourier-transform (FT) mid-infrared, FT-Raman and near-infrared spectrometry. *Journal of Pharmaceutical and Biomedical Analysis*, *13*(4), 409–414.

Li, H.-Q., & Xu, J. (2013). A new correction method for determination on carbohydrates in lignocellulosic biomass. *Bioresource Technology*, *138*, 373–376.

Lipp, M. (1996). Comparison of PLS, PCR and MLR for the quantitative determination of foreign oils and fats in butter fats of several European countries by their triglyceride composition. *Zeitschrift für Lebensmittel-Untersuchung und Forschung*, *202*(3), 193–198.

Mak, C., Yuen, C., Ku, S., & Kan, C. (2006). Changes in surface morphology of Tencel fabric during the fibrillation process. *Journal of the Textile Institute*, *97*(3), 241–246.

Oliver, J. D., Gaborieau, M., Hilder, E. F., & Castignolles, P. (2013). Simple and robust determination of monosaccharides in plant fibers in complex mixtures by capillary electrophoresis and high performance liquid chromatography. *Journal of Chromatography A*, *1291*, 179–186.

Pettersen, R. C. (1984). The chemical composition of wood. *Chemistry of Solid Wood*, *207*, 57–126.

Philip Ye, X., Liu, L., Hayes, D., Womac, A., Hong, K., & Sokhansanj, S. (2008). Fast classification and compositional analysis of cornstover fractions using Fourier transform near-infrared techniques. *Bioresource Technology*, *99*(15), 7323–7332.

Raymond, C. A., & Schimleck, L. R. (2002). Development of near infrared reflectance analysis calibrations for estimating genetic parameters for cellulose content in *Eucalyptus globulus*. *Canadian Journal of Forest Research*, *32*(1), 170–176.

Roggo, Y., Chalus, P., Maurer, L., Lema-Martinez, C., Edmond, A., & Jent, N. (2007). A review of near infrared spectroscopy and chemometrics in pharmaceutical technologies. *Journal of Pharmaceutical and Biomedical Analysis*, *44*(3), 683–700.

Ruffing, T. C., Shi, W. W., Brown, N. R., & Smith, P. M. (2011). Review of United States and international formaldehyde emission regulations for interior wood composite panels. *Wood and Fiber Science*, *43*(1), 21–31.

Schultz, T., & Burns, D. (1990). Rapid secondary analysis of lignocellulose: Comparison of near infrared (NIR) and Fourier transform infrared (FTIR). *Tappi Journal*, *73*(5), 209–212.

Schwanninger, M., Rodrigues, J. C., & Fackler, K. (2011). A review of band assignments in near infrared spectra of wood and wood components. *Journal of Near Infrared Spectroscopy*, *19*(5), 287–308.

Senter, H. F. (2008). Applied linear statistical models. *Journal of the American Statistical Association*, *103*(482), 880.

Sjoblom, E., Johnsson, B., & Sundstrom, H. (2004). Optimization of particleboard production using NIR spectroscopy and multivariate techniques. *Forest Products Journal*, *54*, 71–75.

Sluiter, A., Hames, B., Ruiz, R., Scarlata, C., Sluiter, J., Templeton, D., et al. (2008). Determination of structural carbohydrates and lignin in biomass. *Laboratory Analytical Procedure*, 1–15.

Tsuchikawa, S. (2007). A review of recent near infrared research for wood and paper. *Applied Spectroscopy Reviews*, *42*(1), 43–71.

Via, B., Fasina, O., & Pan, H. (2011). Assessment of pine biomass density through mid-infrared spectroscopy and multivariate modeling. *BioResources*, *6*(1), 807–822.

Via, B. K. (2010). Prediction of oriented strand board wood strand density by near infrared and Fourier transform infrared reflectance spectroscopy. *Journal of Near Infrared Spectroscopy*, *18*(6), 491–498.

Via, B. K., Adhikari, S., & Taylor, S. (2013). Modeling for proximate analysis and heating value of torrefied biomass with vibration spectroscopy. *Bioresource Technology*, *133*, 1–8.

Via, B. K., Shupe, T. F., Groom, L. H., Stine, M., & So, C.-L. (2003). Multivariate modelling of density, strength and stiffness from near infrared spectra for mature, juvenile and pith wood of longleaf pine (*Pinus palustris*). *Journal of Near Infrared Spectroscopy*, *11*(5), 365–378.

Via, B. K., Zhou, C., Acquah, G., Jiang, W., & Eckhardt, L. (2014). Near infrared spectroscopy calibration for wood chemistry: Which chemometric technique is best for prediction and interpretation? *Sensors*, *14*(8), 13532–13547.

Viscarra Rossel, R., Walvoort, D., McBratney, A., Janik, L. J., & Skjemstad, J. (2006). Visible, near infrared, mid infrared or combined diffuse reflectance spectroscopy for simultaneous assessment of various soil properties. *Geoderma*, *131*(1), 59–75.

Weinstock, I. A., Atalla, R. H., Reiner, R. S., Moen, M. A., Hammel, K. E., Houtman, C. J., et al. (1997). A new environmentally benign technology for transforming wood pulp into paper. Engineering polyoxometalates as catalysts for multiple processes. *Journal of Molecular Catalysis A: Chemical*, *116*(1), 59–84.

Williams, P. C., & Sobering, D. (1993). Comparison of commercial near infrared transmittance and reflectance instruments for analysis of whole grains and seeds. *Journal of Near Infrared Spectroscopy*, *1*(1), 25–32.

Yeh, T.-F., Yamada, T., Capanema, E., Chang, H.-M., Chiang, V., & Kadla, J. F. (2005). Rapid screening of wood chemical component variations using transmittance near-infrared spectroscopy. *Journal of Agricultural and Food Chemistry*, *53*(9), 3328–3332.

Zhang, Y., Cong, Q., Xie, Y., & Zhao, B. (2008). Quantitative analysis of routine chemical constituents in tobacco by near-infrared spectroscopy and support vector machine. *Spectrochimica Acta, A: Molecular and Biomolecular Spectroscopy*, *71*(4), 1408–1413.